Applied Physics Letters

Tungsten-doped $Ge_2Sb_2Te_5$ phase change material for high-speed optical switching devices

Cite as: Appl. Phys. Lett. **116**, 131901 (2020); https://doi.org/10.1063/1.5142552
Submitted: 16 December 2019 . Accepted: 16 March 2020 . Published Online: 01 April 2020

Pengfei Guo, Joshua A. Burrow, Gary A. Sevison, Heungdong Kwon, Christopher Perez, Joshua R. Hendrickson, Evan M. Smith, Mehdi Asheghi, Kenneth E. Goodson, Imad Agha, and Andrew M. Sarangan

View Online Export Citation CrossMark

ARTICLES YOU MAY BE INTERESTED IN

Comparison of Sb, As, and P doping in Cd-rich CdTe single crystals: Doping properties, persistent photoconductivity, and long-term stability
Applied Physics Letters **116**, 132102 (2020); https://doi.org/10.1063/5.0004883

Properties of bulk scandium nitride crystals grown by physical vapor transport
Applied Physics Letters **116**, 132103 (2020); https://doi.org/10.1063/1.5141808

Spin-transport in superconductors
Applied Physics Letters **116**, 130501 (2020); https://doi.org/10.1063/1.5138905

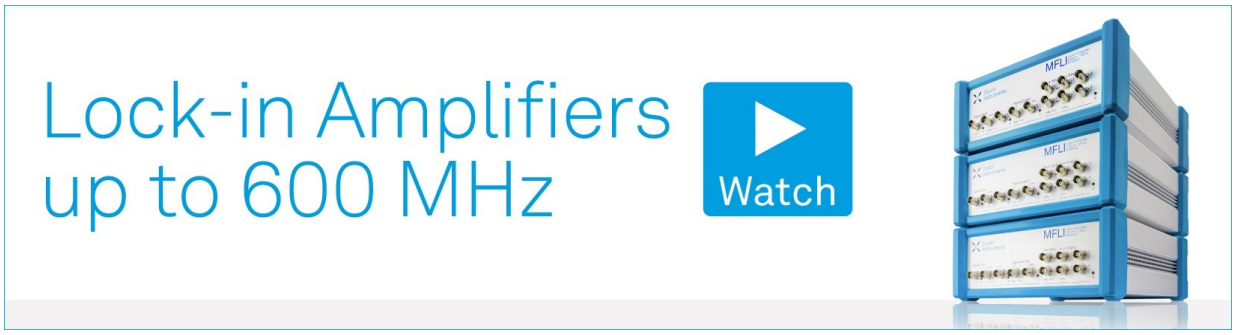

© 2020 Author(s).

Applied Physics Letters ARTICLE scitation.org/journal/apl

Tungsten-doped $Ge_2Sb_2Te_5$ phase change material for high-speed optical switching devices

Cite as: Appl. Phys. Lett. **116**, 131901 (2020); doi: 10.1063/1.5142552
Submitted: 16 December 2019 · Accepted: 16 March 2020 ·
Published Online: 1 April 2020

View Online Export Citation CrossMark

Pengfei Guo,[1] Joshua A. Burrow,[1] Gary A. Sevison,[1,2] Heungdong Kwon,[3] Christopher Perez,[3] Joshua R. Hendrickson,[2] Evan M. Smith,[2,4] Mehdi Asheghi,[3] Kenneth E. Goodson,[3] Imad Agha,[1,5] and Andrew M. Sarangan[1,a)]

AFFILIATIONS

[1]Department of Electro-Optics and Photonics, University of Dayton, Dayton, Ohio 45469, USA
[2]Air Force Research Laboratory, Wright-Patterson AFB, Ohio 45433, USA
[3]Department of Mechanical Engineering, Stanford University, Stanford, California 94305, USA
[4]KBR, Beavercreek, Ohio 45431, USA
[5]Department of Physics, University of Dayton, Dayton, Ohio 45469, USA

[a)]Author to whom correspondence should be addressed: asaragan1@udayton.edu

ABSTRACT

The large impedance mismatch between the highly resistive amorphous state and the highly conductive crystalline state of $Ge_2Sb_2Te_5$ is an impediment for the realization of high-speed electrically switched optical devices. In this paper, we demonstrate that tungsten doping can reduce this resistivity contrast and also results in a lower amorphous state resistivity. Additionally, it lowers the contact resistance, improves the optical contrast, and extends the face-centered-cubic state up to 350 °C, with a minimal impact on thermal conductivity.

Published under license by AIP Publishing. https://doi.org/10.1063/1.5142552

Phase-change materials (PCMs) undergo a reversible structural change between amorphous and crystalline states in response to a temperature impulse. Due to the vast difference in optical and electrical properties between these phases, PCMs can be used in random access memory[1] and tunable optical devices.[2,3] While there are many different phase change materials, $Ge_2Sb_2Te_5$ (GST) is the most widely studied composition because of its fast crystallization speed, reversible phase transition, and good endurance over a wide temperature range. However, there are some key practical challenges in applying it to high speed switching devices. First, GST has an extremely large resistivity in the amorphous state (several hundred Ω m),[4] which means a large voltage or a long pulse duration is required to dissipate sufficient energy in the device to induce the phase transition to the crystalline state. The second challenge comes from the large disparity in electrical impedance between the amorphous and crystalline states. It is not possible to simultaneously impedance match the driving circuitry for both states. In optical switching applications, it is the optical contrast that is most important, while the electrical impedance is ideally kept constant. Hence, this work is motivated by the need to reduce the electrical contrast between the two phases of GST while preserving its optical contrast.

Doping is one of the most effective and simplest methods to modify the properties of phase change materials. Various dopants have been examined in the last few years to improve the electrical or optical properties of GST. These include nitrogen,[5] carbon,[6] oxygen,[7] tin,[8] aluminum,[9] silver,[10] titanium,[11] nickel,[12] arsenic,[13] and copper.[14] All these studies have been focused on adding dopants into the GST host to modify its electrical resistivity. None of them have been aimed at reducing the resistivity *contrast* between the amorphous and crystalline states. Guo *et al.*[15,16] studied the Raman spectra and dielectric function of tungsten-doped GST with different tungsten concentrations. Cheng *et al.* showed that tungsten-doped GST has a higher crystallization temperature with high switching speed. The electrical set pulse was 10 ns, which is faster than the 50 ns required for undoped GST.[17] Despite these previous studies, a systemic examination of tungsten-doped GST (hereafter GST-W) has been lacking. The objective of this paper is to examine the electrical, optical, structural, and thermal characteristics of GST-W and quantify its beneficial properties compared to undoped-GST for electrically driven optical switching devices.

The thin films used in this work were deposited on silica glass and silicon substrates [silica glass for electrical and XRD work and Si(100) for thermal conductivity measurements]. The depositions were done by co-sputtering from dual 3-in. circular magnetron cathodes. The cathode containing the GST target was energized by a 13.56 MHz

Published under license by AIP Publishing

RF source, and the tungsten containing cathode was supplied from a DC source. The RF discharge power on the GST target was maintained at 100 W, and the DC power on the tungsten target was set at various values to achieve the desired tungsten doping level. The 4% doping used in this study requires an extremely small deposition rate from tungsten, which would require biasing the target very close to its sputter threshold. In order to ensure the stability and repeatability of the deposition process, we maintained the DC power at 65 W (which is much higher than that required for 4% doping), and we utilized a physical mesh between the target and the substrate to reduce the tungsten accumulation rate on the substrate.

The thicknesses of the films were measured using a stylus surface profilometer. The tungsten concentration in the co-sputtered film was obtained by using an EDAX Genesis 2000 energy dispersive spectroscopy (EDS) system. The resistivity and the contact resistance were measured using a four-point probe and a two-point-patterned electrode structure, respectively. The XRD measurement was carried out using a PAN Analytical Expert Pro MPD in the range of 2θ from 15° to 65°. A sputtered tri-layer structure Pt/TiN/GST or GST-W/Si(100) substrate was used to study the thermal conductivity of the films. The refractive index measurement was performed using spectroscopic ellipsometry (JA Woollam, V-Vase) and fitted between 270 nm and 3000 nm.

The resistivity values of the GST and GST-W films were measured using a four-point probe after annealing them at several discrete temperatures. A series of experiments were conducted to identify the lowest resistivity contrast between the amorphous and crystalline states. More specifically, by setting the RF power on the GST target at 100 W and fine tuning the DC power on the tungsten target, as well as placing different mesh sizes, we were able to achieve the lowest resistivity contrast at a doping concentration of 4%. The concentration value was determined using EDS by taking the average from three spots on the film. The results show an average ratio of Ge:Sb:Te:W = 21:21:54:4 at. % for the tungsten doped film. The standard deviations for Ge, Sb, Te, and W in the measurements were 0.65, 0.32, 0.2, and 0.5, respectively.

In Fig. 1, we can identify two obvious drops in resistivity for the undoped GST between 150 °C and 160 °C and between 275 °C and 300 °C. The first sharp transition near 150 °C corresponds to the amorphous to face-centered-cubic (fcc) phase transition, and the second transition is the fcc to hexagonal close-packed (hcp) phase transition. For the GST-W film, we can see that the phase change occurs at around 225 °C, which agrees with the previously reported results.[17] The resistivity of amorphous GST-W is lower than that of the undoped GST by more than three orders of magnitude. But the resistivity of the crystalline GST-W remains higher than that of the undoped GST. As a result, the change in electrical impedance is only first-order of magnitude for GST-W, while it is more than four orders for the undoped GST. This is one of the key characteristics that enable us to reduce the electrical voltage required to switch phases and provide a better impedance matching with the driving electronics.

We note that the atomic radius of tungsten (210 pm) is close to that of Ge (211 pm), which makes it likely that tungsten atoms act as substitutional impurities in the crystal lattice of GST. As such, it is likely that tungsten acts as an acceptor for germanium, making it a p-type dopant. This hypothesis was verified by measuring the electrical polarity of the films using the hot probe method[18,19] and was found to be p-type.

One of the challenges in GST devices is the contact resistance. In particular, the contact resistance between a metal electrode and the amorphous GST is typically very high, which introduces challenges during electrical switching. Based on the lower amorphous state resistivity of GST-W, we expect the contact resistance of GST-W to also become smaller. To confirm this, the contact resistance between GST (doped and undoped) and a tungsten electrode was measured using the Transfer Length Method (TLM).[20] The tungsten electrodes were created on GST and GST-W films by photolithography, sputter deposition, and lift-off. Figure 2 shows the total resistance of the films. The contact resistance was calculated as half the y-intercept from the linear trend line. This measurement demonstrates that the contact resistance declines by nearly four orders of magnitude due to tungsten doping.

Figure 3 shows the XRD characterization results of the GST and GST-W films on silica glass annealed at different temperatures. The as-deposited films exhibit no identifiable peaks in the XRD data, confirming that they are amorphous. The wide undulance around 29° may be due to the [200] peak.[11] After annealing the GST samples at 170 °C, the film exhibits a metastable fcc state shown by the [111],

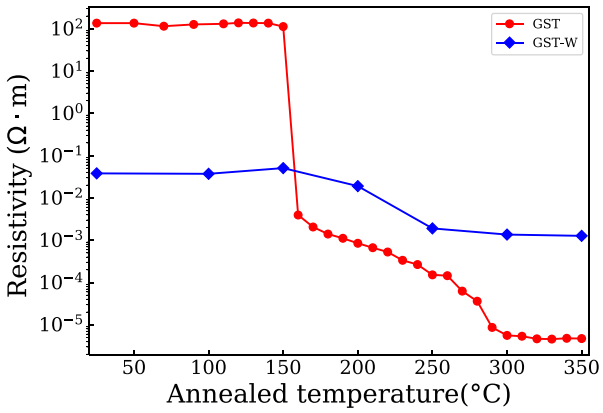

FIG. 1. Relationship between film resistivity and annealing temperature of the undoped GST (red circles) and GST-W (blue diamonds) films.

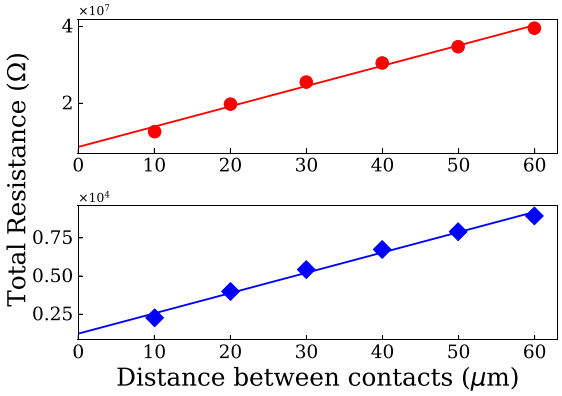

FIG. 2. Contact resistance measurement using the transfer length method (TLM) for the GST (red circles) and GST-W (blue diamonds) film. The markers represent the mean data points collected, and lines are the linear fit to the data points.

Published under license by AIP Publishing

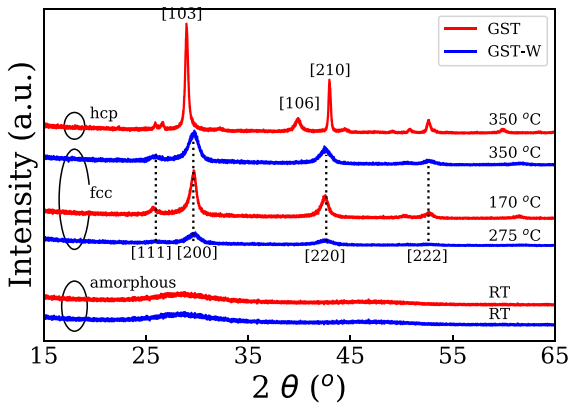

FIG. 3. XRD pattern of GST and GST-W films for the as-deposited state at room temperature (RT) (bottom), after annealing at 170 °C for GST and 275 °C for GST-W (middle), and after annealing at 350 °C (top). The curves have been offset for clarity.

[200], [220], and [222] peaks, which are typical for the NaCl like cubic cell structure.[21] At 350 °C, new peaks emerge in the crystal structure of GST, which correspond to the hexagonal state.[22] Since Fig. 1 shows a leveling off of the resistivity data at around 250 °C, the GST-W sample was annealed at 275 °C and 350 °C to investigate its structural character in this range. The diffraction peaks of GST-W at 275 °C are very similar to those of the GST film annealed at 170 °C. This confirms that the GST-W film is still in the fcc state at 275 °C. Most interestingly, the diffraction peaks of the GST-W film annealed at 350 °C also align very well with the fcc state. The peak intensities are also higher. Therefore, we can conclude that GST-W at 350 °C is still in the fcc state, with a higher degree of fcc crystallinity than at 275 °C. This feature allows the useful (and reversible) fcc state to extend to much higher temperatures than the undoped GST. Another notable aspect is the change in the thickness that occurs during phase transition. We measured the film thicknesses of GST and GST-W when they were annealed to 200 °C and 300 °C, respectively. The results show the GST film thickness decreased by about 5%, which is close to the previously reported value,[23] while the GST-W film increased by about 2%.

Since the phase change is initiated mainly through thermal interactions, understanding the effects of doping on thermal transport becomes crucial. Time-domain thermoreflectance (TDTR) is an ultrafast optical pump-probe technique for measuring the thermophysical properties of both bulk and thin film materials.[24,25] The measured thermoreflectance data are fit to the solution of a 3D heat diffusion model for a multi-layer stack of materials, and the unknown thermophysical properties of interest are used as parameters to converge the measurement and theory.[26]

A lithographically patterned platinum resistive heater on a Si/SiO_2 substrate was used as a compact heating stage within our cryostat. By using a high voltage power source, the samples were subjected to temperatures of up to 335 °C, which were measured using a calibrated thermocouple affixed to the surface of the sample during the TDTR experiment. To prevent intermixing between the Pt transducer and the GST (GST-W) at high temperatures, a 23.5 nm TiN capping layer was deposited in between. The properties of the Pt layer, the TiN capping layer, and the Si substrate were determined from independent measurements or adopted from the literature.[27–29] The volumetric heat capacity of both GST and GST-W was taken to be 1.3 J cm^{-3} K^{-1}, and the thermal conductivity of TiN was assumed to be 11 W m^{-1} K^{-1} based on literature estimates.[30,31] Beginning from their amorphous states at room temperature, the effective thermal conductivities of both the GST and GST-W samples were extracted *in situ* as a function of temperature by heating the samples continuously at approximately 1 K/min, as shown in Fig. 4.

The measured thermal conductivity of GST-W shows a gradual increase between 150 °C and 250 °C, corresponding to its amorphous to fcc phase transition.[32] The room-temperature value of both GST and GST-W was 0.16 ± 0.01 W m^{-1} K^{-1}, agreeing well with the literature for amorphous GST.[24,32] Beyond 250 °C, the tungsten doped GST possesses a slightly greater thermal conductivity at any given temperature until its fcc value of 1.30 ± 0.05 W m^{-1} K^{-1} is achieved. This places the thermal conductivity of tungsten doped GST within the experimental uncertainty of its undoped counterpart (1.20 ± 0.04 W m^{-1} K^{-1}), demonstrating that the thermal conductivity of the tungsten doped GST is nearly the same as that of undoped GST.

Since the goal of this work was to modify GST such that its electrical contrast is reduced without adversely affecting its optical contrast, spectroscopic ellipsometry measurements were carried out on the doped and undoped GST films to verify their optical dispersion. The complex refractive indices of these films were obtained by modeling data taken using variable angle spectroscopic ellipsometry (JA Woollam, V-Vase) between 270 nm and 3000 nm. The model fits a series of Gaussian oscillators to account for various absorption regions as well as a Cauchy term. A surface roughness layer (EMA model of 50% void and 50% GST model) was also allowed to fit, which indicated a roughness between 1 and 2 nm on the tungsten doped samples.

In order to cover all the states, we examined the refractive index data for the as-deposited GST (amorphous), as-deposited GST-W (amorphous), GST annealed at 170 °C (fcc) and 350 °C (hcp), and GST-W annealed at 350 °C (fcc). The results are shown in Fig. 5. In the wavelength range of interest (above 1 μm), the refractive index (n) increases by about 2.0 due to the amorphous-to-fcc crystallization for

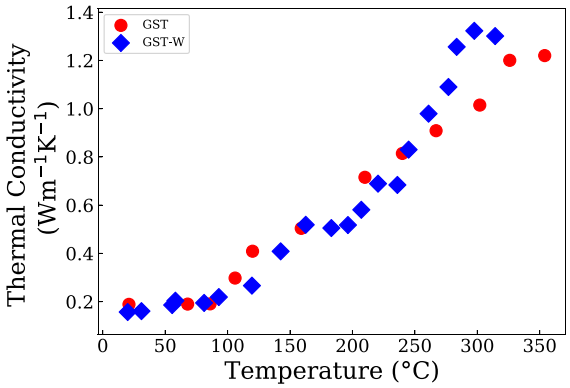

FIG. 4. Evolution of thermal conductivity as a function of temperature for undoped GST (red circles) and GST-W (blue diamonds). The *in situ* data were taken during continuous heating to 355 °C. The Pt transducer layer failed at approximately 315 °C for the GST-W samples, preventing further measurements after this temperature.

Published under license by AIP Publishing

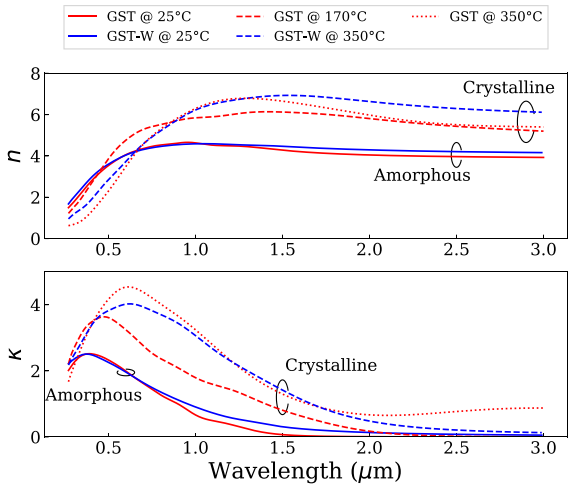

FIG. 5. Wavelength dispersion of the real (n) and imaginary (κ) part of the refractive index of GST (red) and GST-W (blue) films. The refractive index of the film in the amorphous, fcc, and hcp states is denoted by the solid, dashed, and dotted curves, respectively.

both the doped and undoped films. GST-W in the fcc state exhibits a higher refractive index and a slightly smaller extinction coefficient (κ) in the longer wavelength range compared to the undoped GST, making it a better material for optical switching applications. We also note that at wavelengths below 2 μm, the extinction coefficient of GST-W annealed at 350 °C shows similarities with GST annealed at 350 °C. This extension of GST-W at 350 °C with the fcc state provides a good platform for optical driven switching devices with electrical readout, for both crystallization and re-amorphization. More importantly, above 2 μm, the GST-W sample annealed at 350 °C shows very small optical loss, close to zero, while the undoped GST shows a much higher extinction in the longer wavelength range. This feature makes GST-W a good material for designing broadband low loss optical phase modulators above 2 μm.

In conclusion, we have demonstrated that the resistivity contrast of GST can be reduced to just one order of magnitude by introducing 4% tungsten into the GST host material. The amorphous resistivity of GST-W was lowered by over three orders of magnitude, while the crystalline (fcc) resistivity increased by nearly one order of magnitude. The TLM measurement showed that the contact resistance was also reduced by nearly four orders of magnitude. The XRD results show that GST-W remains in the fcc structure up to 350 °C, whereas undoped GST switches to the hcp state beyond 300 °C. Since hcp is much more difficult to reverse than the fcc state, this characteristic of GST-W allows for a wider temperature range of operation. Spectroscopic ellipsometry results demonstrate that GST-W has a larger and less-dispersive refractive index contrast compared to undoped GST. The extinction coefficient is also lower for GST-W, especially at longer wavelengths. As a result, we conclude that GST-W is among the best-suited material to date for application in electrically switched high-speed optical devices.

This work was supported by the National Science Foundation under Grant Nos. 1710273 and 1709200, the University of Dayton graduate school, and AFOSR (15RYCOR159). The authors thank Zachary Biegler for the XRD measurements.

REFERENCES

[1] S. Raoux, G. W. Burr, M. J. Breitwisch, C. T. Rettner, Y.-C. Chen, R. M. Shelby, M. Salinga, D. Krebs, S.-H. Chen, and H.-L. Lung, IBM J. Res. Dev. **52**, 465 (2008).
[2] J. Hendrickson, H. Liang, R. Soref, and J. Mu, Appl. Opt. **54**, 10698 (2015).
[3] A. Sarangan, J. Duran, V. Vasilyev, N. Limberopoulos, I. Vitebskiy, and I. Anisimov, IEEE Photonics J. **10**, 1 (2018).
[4] P. Guo, A. M. Sarangan, and I. Agha, Appl. Sci **9**, 530 (2019).
[5] H. Seo, T.-H. Jeong, J.-W. Park, C. Yeon, S.-J. Kim, and S.-Y. Kim, Jpn. J. Appl. Phys., Part 1 **39**, 745 (2000).
[6] X. Zhou, L. Wu, Z. Song, F. Rao, M. Zhu, C. Peng, D. Yao, S. Song, B. Liu, and S. Feng, Appl. Phys. Lett. **101**, 142104 (2012).
[7] S. Privitera, E. Rimini, and R. Zonca, Appl. Phys. Lett. **85**, 3044 (2004).
[8] M. L. Lee, K. T. Yong, C. L. Gan, L. H. Ting, S. B. M. Daud, and L. Shi, J. Phys. D **41**, 215402 (2008).
[9] G. Wang, X. Shen, Q. Nie, R. Wang, L. Wu, Y. Lv, F. Chen, J. Fu, S. Dai, and J. Li, J. Phys. D **45**, 375302 (2012).
[10] M. Popescu, A. Velea, F. Sava, A. Lőrinczi, A. Tomescu, C. Simion, E. Matei, G. Socol, I. Mihailescu, A. Andonie *et al.*, Phys. Status Solidi A **207**, 516 (2010).
[11] S. Wei, H. Zhu, K. Chen, D. Xu, J. Li, F. Gan, X. Zhang, Y. Xia, and G. Li, Appl. Phys. Lett. **98**, 231910 (2011).
[12] P. Guo, J. A. Burrow, G. A. Sevison, A. Sood, M. Asheghi, J. R. Hendrickson, K. E. Goodson, I. Agha, and A. Sarangan, Appl. Phys. Lett. **113**, 171903 (2018).
[13] V. E. Madhavan, M. Carignano, A. Kachmar, and K. Sangunni, Sci. Rep. **9**, 12985 (2019).
[14] K. Ding, K. Ren, F. Rao, Z. Song, L. Wu, B. Liu, and S. Feng, Mater. Lett. **125**, 143 (2014).
[15] S. Guo, Z. Hu, X. Ji, T. Huang, X. Zhang, L. Wu, Z. Song, and J. Chu, RSC Adv. **4**, 57218 (2014).
[16] S. Guo, X. Ding, J. Zhang, Z. Hu, X. Ji, L. Wu, Z. Song, and J. Chu, Appl. Phys. Lett. **106**, 052105 (2015).
[17] X. Cheng, F. Mao, Z. Song, C. Peng, and Y. Gong, Jpn. J. Appl. Phys., Part 1 **53**, 050304 (2014).
[18] G. Golan, A. Axelevitch, B. Gorenstein, and V. Manevych, Microelectron. J. **37**, 910 (2006).
[19] T. Kato and K. Tanaka, Jpn. J. Appl. Phys., Part 1 **44**, 7340 (2005).
[20] R. Janoch, A. M. Gabor, A. Anselmo, and C. E. Dubé, in *2015 IEEE 42nd Photovoltaic Specialist Conference (PVSC)* (IEEE, 2015), pp. 1–6.
[21] D.-H. Shin, M.-J. Song, J.-W. Kim, G.-H. Kim, K. Hong, and D.-S. Lim, Jpn. J. Appl. Phys., Part 1 **53**, 031402 (2014).
[22] Z. Xu, B. Liu, Y. Chen, D. Gao, H. Wang, Y. Xia, Z. Song, C. Wang, N. Zhu, J. Ren *et al.*, ECS Solid State Lett. **4**, P105 (2015).
[23] J. Xu, C. Qi, L. Chen, L. Zheng, and Q. Xie, AIP Adv. **8**, 055006 (2018).
[24] C. Ahn, S. W. Fong, Y. Kim, S. Lee, A. Sood, C. M. Neumann, M. Asheghi, K. E. Goodson, E. Pop, and H. S. Wong, Nano Lett. **15**, 6809 (2015).
[25] A. Sood, J. Cho, K. D. Hobart, T. I. Feygelson, B. B. Pate, M. Asheghi, D. G. Cahill, and K. E. Goodson, J. Appl. Phys. **119**, 175103 (2016).
[26] D. G. Cahill, Rev. Sci. Instrum. **75**, 5119 (2004).
[27] G. A. Slack and C. J. Glassbrenner, Phys. Rev. **134**, A1268 (1964).
[28] J. Arblaster, Platinum Met. Rev. **38**, 119 (1994).
[29] M. W. Chase, Jr., *NIST-JANAF Thermochemical Tables*, 4th edition, Monograph 9, Parts I and II (American Institute of Physics, 1998).
[30] D. S. Suh, C. Kim, K. H. Kim, Y. S. Kang, T. Y. Lee, Y. Khang, T. S. Park, Y. G. Yoon, J. Im, and J. Ihm, Appl. Phys. Lett. **96**, 142112 (2010).
[31] P. Zalden, K. S. Siegert, S. Rols, H. E. Fischer, F. Schlich, T. Hu, and M. Wuttig, Chem. Mater. **26**, 2307 (2014).
[32] H.-K. Lyeo, D. G. Cahill, B.-S. Lee, J. R. Abelson, M.-H. Kwon, K.-B. Kim, S. G. Bishop, and B.-K. Cheong, Appl. Phys. Lett **89**, 151904 (2006).

Published under license by AIP Publishing